Electrodynamic effects in plasmonic nanolenses

Jianhua Dai,[1] Frantisek Čajko,[1] Igor Tsukerman,[1] and Mark I. Stockman[2]
[1]*Department of Electrical and Computer Engineering, The University of Akron, Ohio 44325-3904, USA*
[2]*Department of Physics and Astronomy, Georgia State University, Atlanta, Georgia 30303, USA*
(Received 19 October 2007; revised manuscript received 15 January 2008; published 12 March 2008)

Full electrodynamic analysis of self-similar cascades of plasmonic nanospheres (nanolenses) that exhibit nanofocusing is performed. Electrodynamic resonances are identified and a significant local field enhancement (by a factor of hundreds) is found for different sizes and fractal ratios of the cascade system, and for different polarizations and directions of incidence of the excitation radiation. Supporting the earlier findings, the nanofocus ("hottest spot") is found to be located in the gap between the two smallest nanospheres of the cascade. Somewhat surprisingly, field enhancement is maximized when the incoming wave is polarized at an angle to the symmetry axis. The influence of the dielectric substrate on field enhancement is also evaluated. The results obtained show ways to optimize the nanolenses for their applications in spectroscopy and sensing.

DOI: 10.1103/PhysRevB.77.115419 PACS number(s): 42.25.Bs, 41.20.Cv, 42.25.Fx

I. INTRODUCTION

Nano-optics is experiencing a period of explosive growth in both fundamental development and applications, with more important applications foreseeable in the near future. Nanoplasmonics, one of the key directions in nanooptics, deals with electric [surface plasmons (SPs)] and electromagnetic (surface plasmon polaritons) excitations at metal surfaces and metal and/or dielectric interfaces. While the localization radius of electromagnetic waves cannot under normal circumstances be significantly less than their wavelength (the diffraction limit), the SPs, as purely electric oscillations, can localize on the nanometer scale.[1–9] In the framework of macroscopic electromagnetics, the minimum localization length of SPs is determined only by the smallest scale of the nanostructure.[3,4] The nanolocalization is intimately related to the large enhancement of the local plasmonic fields. This enhancement plays a key role in many effects and in multiple applications of nanoplasmonics—specifically, in near-field scanning optical microscopy[9] and detectors of chemical and biological objects.[10–12]

Surface-enhanced Raman scattering (SERS)[13–17] can be singled out as a phenomenon that exhibits the greatest enhancement of all known natural phenomena, which enables Raman spectroscopy of single molecules[18,19] and the observation of the surface-enhanced hyper-Raman scattering.[20] The SERS enhancement coefficient g^R is approximately on the order of the fourth power of the local field enhancement g, $g^R \sim g^4$, where $g=|\mathbf{E}|/|\mathbf{E}_0|$; $\mathbf{E}$ is the local optical electric field, and $\mathbf{E}_0$ is the electric field of the excitation wave (see, e.g., Ref. 21). The estimates obtained from the single-molecule SERS show that the enhancement factor can be as high as $g^R \sim 10^{12}-10^{14}$. From this, it appears that the local field can be enhanced (in the red and near-infrared spectral region) by a factor $g \gtrsim 10^3$. At the same time, electrodynamic computations for realistic models show that the SERS enhancement is still several orders of magnitude lower than the experimental estimates would suggest.[21] One possible explanation is the so-called chemical enhancement due to the amplification of the transition dipole moments of a molecule chemically bound to a metal surface at the junction of silver nanoparticles.[22] *Cascade enhancement*, considered in detail below, has been proposed in Ref. 23 as another possibility of explaining the experimentally observed SERS enhancement via a purely electromagnetic mechanism.

II. CASCADE ENHANCEMENT

Cascade amplification produces high local fields in the gaps between the smallest particles in nanoparticle clusters of *significantly* different sizes. A specific system considered in Ref. 23 is a self-similar cluster of three spherical silver particles aligned along the symmetry axis (Fig. 1). The idea of the cascade enhancement is very simple. The largest nanoparticle has a SP resonance that is not significantly perturbed by smaller particles because their polarizabilities, proportional to their volumes, are much smaller. The local optical field of this large particle is enhanced by a quality factor of the SP resonance Q with respect to the external field $\mathbf{E}_0$. This enhanced local field acts on the smaller particles of the cluster as the excitation field. Then the next, smaller, particle responds in kind and generates a local field enhanced by a factor on the order of Q^2, and so on. Obviously, the nth particle in this enhancement cascade produces amplification by a factor of $\sim Q^n$. The strongest enhanced local field tends to localize in the gap between the two smallest nanoparticles, producing a nanofocus as small as the minimum gap. The quality factor can be estimated as[21] $Q \sim -\mathrm{Re}\,\varepsilon_m/\mathrm{Im}\,\varepsilon_m$, where ε_m is the dielectric permittivity of the metal at the excitation frequency. For silver in the optical range, $Q \gtrsim 10$, which shows that a cascade of just three silver nanoparticles can provide a field enhancement of $g \gtrsim 10^3$, which corresponds to the SERS enhancement $g^R \gtrsim 10^{12}$.

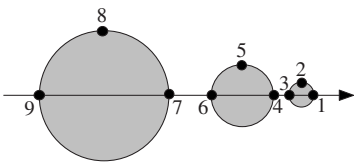

FIG. 1. A cascade of three particles and reference points for field enhancement.

This idea has been confirmed in Ref. 23 for self-similar cascades of three, five, and six nanospheres, where the ratio of the sizes of the neighboring nanospheres in the cascade $\kappa=R_n/R_{n-1}=1/3$. The gaps in this cascade also form a geometric series with the same ratio $d_n/d_{n-1}=\kappa$, where d_n is the surface-to-surface gap between nth and $(n-1)$th nanospheres. Depending on this ratio, the enhancement predicted for a cluster of three nanospheres was in the range of $g^R=1200-600$ for the range of the ratios $d_n/R_n=0.3-0.6$. For a symmetric cascade of six nanospheres, the enhancement was computed to be approximately two times higher. The numerical computations in Ref. 23 have been carried out under the quasistatic approximation, which is valid only if the size of the system is much smaller than all relevant electromagnetic lengths, in particular, the reduced wavelength $\lambda\!\!\!^{-}=c/\omega$, where c is the speed of light and ω is the optical frequency. However, the most restrictive of these applicability conditions is $R_1 \lesssim l_s$, where R_1 is the radius of the largest nanosphere, and l_s is the skin depth, which is less than 30 nm for plasmonic metals in the optical range. This condition is not fully satisfied in Ref. 23.

A separate source of corrections originates at the *minimum* length scale of the system due to the local optical fields rapidly changing in space. This leads to spatial dispersion of the dielectric responses and related Landau damping that limit the nanolocalization of energy[24,25] (see also Ref. 26). Note that often these effects are taken into account by simply increasing the dephasing collision rate γ of electrons as $\gamma \rightarrow \gamma + Av_F/a$, where v_F is the electron velocity at the Fermi surface, a is a characteristic size of the system, and $A \sim 1$ is a dimensionless constant.[27,28] Actually, effects associated with small dimensions of the particles are due to the nonlocality of both real and imaginary parts of the dielectric function (Landau damping) and do not reduce to the increase of the electron scattering rate. There is substantial experimental evidence that these effects depend strongly on the geometry of nanoparticles. For instance, thin metal-dielectric nanoshells do not show any significant impact of the increased electron scattering rates: there is no discernible spectral broadening of the plasmonic resonances.[29] Because of that, and also because there is currently no theory satisfactorily incorporating the dielectric-response nonlocality into nanoplasmonics, we will not consider such effects at this time.

III. PHYSICAL ASSUMPTIONS AND THE MODEL

It has been noted in the literature that there may be some corrections to the computation results due to both the electrodynamic effects and the nonlocality (Landau damping).[23] Electrodynamic effects have been reported to result in correction factors on the order of 2 for the maximum value of the electric field.[30] However, as argued in Ref. 31, the grid size in the finite-difference time-domain simulation of Ref. 30 was too coarse to accurately represent the rapid variations of the local field at the focus of the nanolens. The objective of this paper is to analyze the impact of electrodynamic effects on the nanofocusing of the optical field more accurately. For this purpose, we use adaptive finite element analysis, one of the most robust numerical techniques available. Our simulations are performed in the frequency domain, which is a straightforward and reliable approach.

We shall assume (as was done in Ref. 23) that, to a reasonable degree of approximation, the permittivity of the particles is equal to its bulk value for silver.[32] In the specific example considered in Ref. 23, the radii of the silver particles are 45, 15, and 5 nm, with the air gaps of 9 and 3 nm. Under the quasistatic approximation, the maximum field enhancement is calculated to occur in the near ultraviolet at $\hbar\omega=3.37$ eV, with the corresponding wavelength of ~ 367.9 nm.

The optical electric field can be split up into the excitation field $\mathbf{E}_0$ and the scattered field $\mathbf{E}_s$ that vanishes at infinity: $\mathbf{E}=\mathbf{E}_0+\mathbf{E}_s$. The governing equation is

$$\nabla \times \nabla \times \mathbf{E}_s - k_0^2 \epsilon \mathbf{E}_s = -(\nabla \times \nabla \times \mathbf{E}_0 - k_0^2 \epsilon \mathbf{E}_0), \quad (1)$$

where $k_0=\omega/c$ is the wave number in free space. The relative dielectric permittivity is $\epsilon=\varepsilon_m(\omega)$ in metal and $\epsilon=1$ in a vacuum. The Maxwell boundary conditions are implied at the metal-dielectric interfaces describing the interfacial charges and currents. In our computations, the incident field $\mathbf{E}_0$ is always a plane wave with the amplitude normalized to unity. In the quasistatic limit, the governing continuity equation is written for the total electrostatic potential $\phi=\phi_0+\phi_s$ that is presented as a sum of the excitation field (external) potential ϕ_0 and the scattered field potential ϕ_s exactly the same way as the electric field is,

$$\nabla \cdot (\epsilon \nabla \phi_s) = -\nabla \cdot (\epsilon \nabla \phi_0), \quad (2)$$

where $\phi_0(\mathbf{r})$ is the applied potential corresponding to the uniform unity electric field in the vicinity of the system.

IV. NUMERICAL SIMULATION AND RESULTS

Our numerical simulations are based on the finite element method (FEM) with Eqs. (1) or (2) rewritten in the weak (variational) form. The Maxwell boundary conditions on the surfaces are automatically satisfied by the solution of this variational problem. The mathematical details of this approach are well known (e.g., Refs. 33, 34, and 36). The electrostatic problem is solved numerically for the *total* potential ϕ. We use the commercial software packages HFSS™ by An-

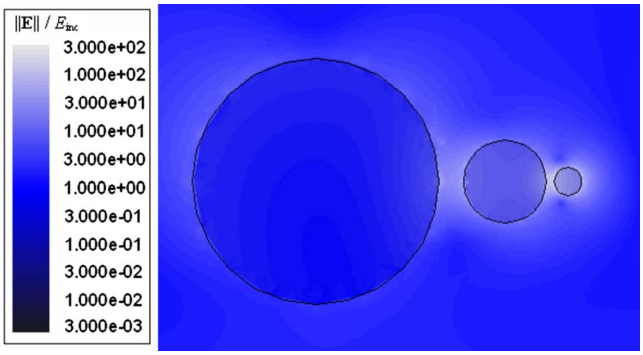

FIG. 2. (Color online) Electric field enhancement factor around the cascade of three plasmonic spheres.

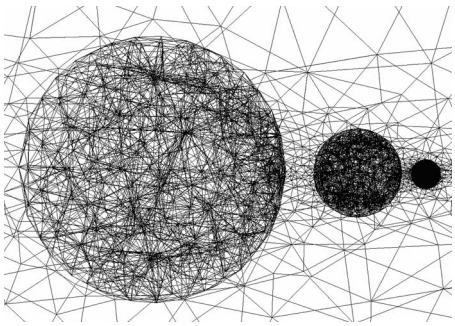

FIG. 3. A sample HFSS™ mesh around the cascade. (hybrid 2D-3D rendition of the 3D mesh used for visual clarity.)

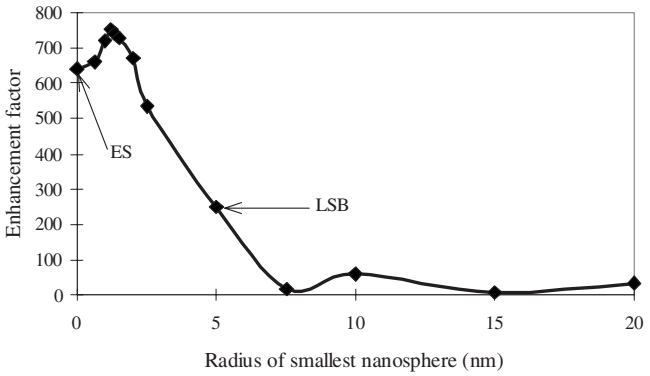

FIG. 4. Maximum field enhancement vs radius of the smallest particle. All dimensions of the system are scaled proportionately. (LSB: dimensions as in the specific example in Ref. 23; the radius of the smallest particle 5 nm. ES: the electrostatic limit.)

soft Corp. for electrodynamic analysis and FEMLAB™ (COMSOL Multiphysics) in the electrostatic case. Both of these packages are FEM based: second-order triangular nodal elements for the electrostatic problem and tetrahedral edge elements with 12 degrees of freedom for wave analysis. The HFSS employs automatic adaptive mesh refinement for higher accuracy and either radiation boundary conditions or perfectly matched layers to truncate the unbounded domain.

To assess the numerical accuracy, we first considered a single particle of radius from 5 to 60 nm. In this range, for the electric field computed at the surface, the differences between the Mie theory[35] and HFSS field values are within 1.2%–3.5% for a dielectric particle with $\epsilon=10$ and within 3.4%–6.3% for a silver particle with $\epsilon_s=-2.74+0.232i$.

This agreement allowed us to proceed to the simulation of particle cascades. A sample distribution of the amplitude of the electric field (as a reminder, the amplitude of the incident field is normalized to unity) in the the cross section of the cascade is shown in Fig. 2. The incident wave is polarized along the axis of the cascade and propagates in the downward direction.

A fragment of a typical FE mesh is shown in Fig. 3. The total number of tetrahedral elements in the computational domain is 99 168. A salient advantage of FEM, as compared with finite-difference methods, is that the mesh is geometrically conforming and represents the curved boundaries accurately. Automatic adaptive mesh refinement leads to higher element density in the vicinity of the smallest silver particle. While the tetrahedral mesh is fully three dimensional, for visual clarity a combined two-dimensional–three-dimensional (2D-3D) rendition of the mesh is used in Fig. 3.

We consider four independent combinations of the directions of wave propagation and polarization (left-right and up-down directions are in reference to Fig. 1).

(i) The incident wave propagates from right to left. The electric and magnetic fields are both perpendicular to the axis of the cascade (mnemonic label: $\Leftarrow\perp$).

(ii) Same as above, but the wave impinges from the left (labeled as $\Rightarrow\perp$).

(iii) The direction of propagation and electric field are both perpendicular to the axis of the cascade (labeled as $\Uparrow\perp$).

(iv) The direction of propagation is perpendicular to the axis, and the electric field is parallel to it (labeled as $\Uparrow\|$).

Table I shows the local field magnitudes (i.e., the field enhancement factors) at the reference points for cases (i)–(iv). The "hottest spot," i.e., the point of the maximum enhancement, is indicated in bold and is different in different cases. When the electric field is perpendicular to the axis of the cascade, the local field is amplified by a very modest factor $g<40$. As expected, the enhancement is much greater ($g\approx 250$) in case (iv), when the field and the dipole moments that it induces are aligned along the axis.

The maximum enhancement ($g\approx 250$) in Table I is smaller than the enhancement $g\approx 600$ predicted for this system in the quasistatic approximation in Ref. 23. However, does it imply that electrodynamic effects always reduce the enhancement relative to the quasielectrostatic limit?

To answer this question and to gauge the influence of electrodynamic effects, we consider field enhancement g as a function of the system size by scaling the system proportionally. This scaling is applied across the board to all dimensions: the radii of all nanospheres and the air gaps between them are multiplied by the same factor. In Fig. 4, we show the dependence of the maximum enhancement (for the $\Uparrow\|$ case) as a function of the radius R_3 of the smallest nano-

TABLE I. Field enhancement at the reference points (see Fig. 1) for different directions of propagation and polarization of the incident wave.

Case	Point 1	Point 2	Point 3	Point 4	Point 5	Point 6	Point 7	Point 8	Point 9
$\Leftarrow\perp$	5.45	17.3	10.2	9.43	**34.4**	10.7	5.53	10.4	3.21
$\Rightarrow\perp$	6.37	6.49	2.41	1.43	4.17	3.39	3.91	**11.2**	2.00
$\Uparrow\perp$	2.44	8.48	6.65	7.60	**23.3**	8.31	4.69	10.1	2.61
$\Uparrow\|$	90.8	35.9	**250**	146	10.3	70.9	51.9	2.72	6.47

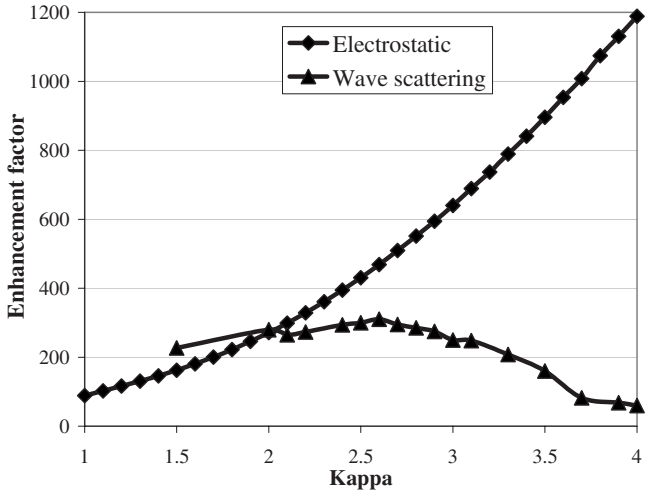

FIG. 5. Maximum field enhancement vs coefficient κ, with the smallest radius of silver particle 5 nm and the smallest air gap 3 nm.

sphere. Note that the original example of Ref. 23 corresponds to $R_3=5$ nm. As we can see, this enhancement depends strongly on the size of the system for $R_3>3$ nm. It shows an interference pattern typical for antennas with two zeros at $R_3=7.5$ nm and $R_3=15$ nm, where destructive interference takes place. It does tend to the value $g=630$ found in the quasistatic approximation[23] for $R_3<1$ nm and is close to this value for $R_3\leqslant 2.5$ nm. It exhibits an *electrodynamic* resonance for $R_3=1.2$, with $g\approx 750$, *exceeding* significantly the quasistatic value.

According to Fig. 4, the highest enhancement in the LSB cascade with the fractal ratio $\kappa=3$ occurs when the radii of the silver particles are $R_3=1.2$ nm, $R_2=R_3\times\kappa=3.6$ nm, and $R_1=R_2\times\kappa=10.8$ nm, and the air gaps are 2.16 and 0.72 nm. However, these dimensions are too small to be practical and for the bulk permittivity to be applicable. Therefore in the search for maximum enhancement as a function of the fractal ratio κ, we fix the radius of the smallest silver particle at $R_3=5$ nm and the smallest air gap at $d_3=3$ nm. Under these conditions, the field enhancement as a function of κ is shown in Fig. 5. Note that the vacuum wavelength is still 367.9 nm, and the incident field is polarized parallel to the cascade axis. The highest field enhancement is found at $\kappa\approx 2.6$ and is approximately 25% higher than for the original value $\kappa=3$.

In practice, particularly for optical sensor applications, the particles are likely to be deposited on a substrate. A possible configuration is shown in Fig. 6. The radii of the particles

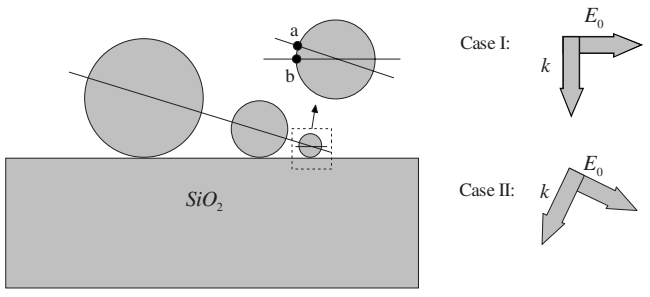

FIG. 6. Particle cascade on a substrate.

TABLE II. Maximum field enhancement factor with and without the substrate.

	With substrate		Without substrate	
	Case I	Case II	Case I	Case II
Point *a*	292	209	338	250
Point *b*	217	154	252	178

and the air gaps are the same as Ref. 23. Two directions of propagation are considered: (I) perpendicular to the substrate and (II) perpendicular to the axis of the cascade.

The silicon dioxide substrate ($\epsilon=1.5$) reduces the maximum field enhancement (Table II), which can be explained by dielectric screening. Field enhancement at point *a*—the point on the smallest nanosphere closest to the middle one—is higher than at point *b*. Interestingly enough, the maximum enhancement is found for the excitation field polarized at an angle to the axis of the cascade (compare cases I and II). The multipole-multicenter calculation for *cylindrical* silver particles (data not shown) yields qualitatively similar results.

V. CONCLUSION

In summary, full electrodynamic computations confirm the qualitative results of the quasistatic analysis:[23] for a self-similar cascade of silver nanoparticles there exists a pronounced nanofocus where the local fields significantly (by a factor of several hundred) enhanced with respect to the excitation field. At the same time, these computations show a wealth of electrodynamic effects related to the total size of the cascade, with both positive and negative resonances possible. At the positive resonance, the enhancement is significantly higher than in the quasistatic case, while at the negative resonances (nodes) it vanishes. The maximum enhancement corresponds to the excitation field polarized at an angle to the axis of the cascade. Hence the size of the system and the excitation polarization are useful variables in the optimization of the optical nanolenses. Another clear possibility to optimize and improve the nanofocusing of optical radiation is to decrease the gaps between the nanoparticles. However, for smaller gaps the continuous electrodynamics approach is not applicable any more. A more comprehensive theory needs to be developed, one that would take into account the nonlocality of optical responses and the electron spillout at scales of 1 nm or less.

ACKNOWLEDGMENTS

The work of J.D., F.C., and I.T. was supported in part by the NSF NIRT Award No. 0304453. The work of M.I.S. was supported by grants from the Chemical Sciences, Biosciences and Geosciences Division of the Office of Basic Energy Sciences, Office of Science, U.S. Department of Energy, Grant No. CHE-0507147 from NSF, and a grant from the US-Israel BSF.

[1] J. R. Krenn, A. Dereux, J. C. Weeber, E. Bourillot, Y. Lacroute, J. P. Goudonnet, G. Schider, W. Gotschy, A. Leitner, F. R. Aussenegg, and C. Girard, Phys. Rev. Lett. **82**, 2590 (1999).
[2] R. Hillenbrand and F. Keilmann, Appl. Phys. B: Lasers Opt. **73**, 239 (2001).
[3] M. I. Stockman, S. V. Faleev, and D. J. Bergman, Phys. Rev. Lett. **87**, 167401 (2001).
[4] M. I. Stockman, S. V. Faleev, and D. J. Bergman, Phys. Rev. Lett. **88**, 067402 (2002).
[5] M. Bosman, V. J. Keast, M. Watanabe, A. I. Maaroof, and M. B. Cortie, Nanotechnology **18**, 16505 (2007).
[6] M. Aeschlimann, M. Bauer, D. Bayer, T. Brixner, F. J. G. d. Abajo, W. Pfeiffer, M. Rohmer, C. Spindler, and F. Steeb, Nature (London) **446**, 301 (2007).
[7] Z. Liu, H. Lee, Y. Xiong, C. Sun, and X. Zhang, Science **315**, 1686 (2007).
[8] I. I. Smolyaninov, Y.-J. Hung, and C. C. Davis, Science **315**, 1699 (2007).
[9] L. Novotny and B. Hecht, *Principles of Nano-Optics* (Cambridge University Press, Cambridge, 2006).
[10] A. J. Haes, S. L. Zou, G. C. Schatz, and R. P. V. Duyne, J. Phys. Chem. B **108**, 109 (2004).
[11] C. R. Yonzon, C. L. Haynes, X. Y. Zhang, J. T. Walsh, and R. P. V. Duyne, Anal. Chem. **76**, 78 (2004).
[12] X. Zhang, M. A. Young, O. Lyandres, and R. P. V. Duyne, J. Am. Chem. Soc. **127**, 4484 (2005).
[13] M. Fleischmann, P. J. Hendra, and A. J. McQuillan, Chem. Phys. Lett. **26**, 163 (1974).
[14] D. L. Jeanmaire and R. P. V. Duyne, J. Electroanal. Chem. Interfacial Electrochem. **84**, 1 (1977).
[15] M. G. Albrecht and J. A. Creighton, J. Am. Chem. Soc. **99**, 5215 (1977).
[16] M. Moskovits, Rev. Mod. Phys. **57**, 783 (1985).
[17] *Surface Enhanced Raman Scattering Physics and Applications*, edited by K. Kneipp, M. Moskovits, and H. Kneipp (Springer-Verlag, Heidelberg, 2006).
[18] K. Kneipp, Y. Wang, H. Kneipp, L. T. Perelman, I. Itzkan, R. R. Dasari, and M. S. Feld, Phys. Rev. Lett. **78**, 1667 (1997).
[19] S. M. Nie and S. R. Emery, Science **275**, 1102 (1997).
[20] J. Kneipp, H. Kneipp, and K. Kneipp, Proc. Natl. Acad. Sci. U.S.A. **103**, 17149 (2006).
[21] M. I. Stockman, in *Surface Enhanced Raman Scattering—Physics and Applications*, edited by K. Kneipp, M. Moskovits, and H. Kneipp (Springer-Verlag, Heidelberg 2006), pp. 47–66.
[22] J. Jiang, K. Bosnick, M. Maillard, and L. Brus, J. Phys. Chem. B **107**, 9964 (2003).
[23] K. Li, M. I. Stockman, and D. J. Bergman, Phys. Rev. Lett. **91**, 227402 (2003).
[24] F. D. M. Haldane, arXiv:cond-mat/0206420 (unpublished).
[25] I. A. Larkin and M. I. Stockman, Nano Lett. **5**, 339 (2005).
[26] M. R. Beversluis, A. Bouhelier, and L. Novotny, Phys. Rev. B **68**, 115433 (2003).
[27] U. Kreibig and L. Genzel, Surf. Sci. **156**, 678 (1985).
[28] U. Kreibig and M. Vollmer, *Optical Properties of Metal Clusters* (Springer, New York, 1995).
[29] C. L. Nehl, N. K. Grady, G. P. Goodrich, F. Tam, N. J. Halas, and J. H. Hafner, Nano Lett. **4**, 2355 (2004).
[30] Z. Li, Z. Yang, and H. Xu, Phys. Rev. Lett. **97**, 079701 (2006).
[31] K. Li, M. I. Stockman, and D. J. Bergman, Phys. Rev. Lett. **97**, 079702 (2006).
[32] P. B. Johnson and R. W. Christy, Phys. Rev. B **6**, 4370 (1972).
[33] P. Monk, *Finite Element Methods for Maxwell's Equations* (Clarendon, Oxford, 2003).
[34] J. Jin, *The Finite Element Method in Electromagnetics* (Wiley, New York/IEEE, New York, 2002).
[35] R. F. Harrington, *Time-Harmonic Electromagnetics Fields* (McGraw-Hill, New York, 1961).
[36] I. Tsukerman, *Computational Methods for Nanoscale Applications: Particles, Plasmons and Waves* (Springer, New York, 2007).